



SMR.959 - 9

MINIWORKSHOP ON STRONG ELECTRON CORRELATIONS
"Disorder and Interaction in Quantum Systems
and Their Classical Analogs"

(1 - 19 July 1996)

"Y₂BaNiO₅: A nearly ideal realization of the S=1 Heisenberg
chain with antiferromagnetic interactions"

Collin Broholm
The Johns Hopkins University
Dept. of Physics & Astronomy
Baltimore, MD 21218
U.S.A.

These are preliminary lecture notes, intended only for distribution to participants.

Y₂BaNiO₅: A nearly ideal realization of the S=1 Heisenberg chain with antiferromagnetic interactions

Guangyong Xu,¹ J. F. DiTusa,² T. Ito,³ K. Oka,³ H. Takagi,⁴ C. Broholm,^{1,5} and G. Aeppli⁶

¹*Department of Physics and Astronomy, the Johns Hopkins University, Baltimore, MD 21218*

²*Department of Physics and Astronomy, Louisiana State University, Baton Rouge, LA 70803*

³*Electrotechnical Lab. Tsukuba 305, Japan*

⁴*ISSP, University of Tokyo, Roppongi, Tokyo 106, Japan*

⁵*National Institute of Standards and Technology, Gaithersburg, MD 20899*

⁶*NEC, 4 Independence Way, Princeton, NJ 08540*

Abstract

We report an inelastic neutron scattering experiment on single crystals of the one dimensional spin-one antiferromagnet Y₂BaNiO₅. The data show that this compound is a nearly ideal material for studying the Haldane conjecture in the Heisenberg limit. In particular, the Haldane gap at $\tilde{q} = \pi$ is almost isotropic, taking on the values of 7.5(1)meV, 8.6(1)meV, and 9.6(1)meV for polarizations parallel to the three principal orthorhombic axes respectively. Inter-chain coupling along the edges of the orthorhombic unit cell is found to be very weak ($J'/J \leq 5 \times 10^{-4}$). Finally, we show that defects in our sample at the 1% level cause visible broadening of the excitation at $\tilde{q} = \pi$.

In 1983 Haldane showed that antiferromagnetic integer spin chains have a singlet ground state separated from a band of triplet excited states by a finite energy gap [1]. Since then a plethora of theoretical [2–4], numerical [5–8] and experimental [9–14] work has confirmed these results and provided additional insight into this unique magnetic phase. Experimental progress in the field is controlled by the discovery of suitable quasi-one-dimensional model systems. The systems studied until now were primarily organic dielectrics, however recently a family of transition metal oxides, $R_2\text{BaNiO}_5$, which also display the Haldane gap was discovered [15]. These materials are leading the research in new directions. For example, partial substitution of a divalent cations such as Ca^{2+} on the normally trivalent Rare Earth (R^{3+}) site places mobile holes on the NiO_5 spin chains with interesting charge and spin dynamics [16,17]. Another fascinating aspect is the antiferromagnetic order which occurs when the R^{3+} ion is magnetic [18]. To understand these novel magnetic phenomena, it is important to know the spin Hamiltonian for Ni^{2+} ions in $R_2\text{BaNiO}_5$. This information is best obtained through studies of the simplest member of the family : Y_2BaNiO_5 . Previous neutron scattering experiments on powder samples and small single crystals of Y_2BaNiO_5 showed a Haldane gap of approximately 9meV [19–21] . Here we report a neutron scattering study of a large Y_2BaNiO_5 single crystal which determines the spin-space anisotropy and interchain coupling in this material [22].

Y_2BaNiO_5 has a body centered orthorhombic structure, space group Immm [23] with lattice parameters $a = 3.7648\text{\AA}$, $b = 5.7550\text{\AA}$, and $c = 11.324\text{\AA}$ at $T=10\text{K}$. We index momentum transfer in the corresponding reciprocal lattice $\mathbf{Q} = h\mathbf{a}^* + k\mathbf{b}^* + l\mathbf{c}^*$. The material contains isolated chains of corner sharing NiO_6 octahedra. Ni atoms within a chain are separated by \mathbf{a} so we use $\tilde{q} = \mathbf{Q} \cdot \mathbf{a} = 2\pi h$ to denote wave vector transfer along the spin chain.

Unpolarized magnetic neutron scattering measures the convolution of a well defined resolution function [24] with the following linear combination of cartesian components of the dynamic spin correlation function [25]:

$$\begin{aligned}
I(\mathbf{Q}, \omega) = & \sin^2 \theta S^{aa}(\mathbf{Q}, \omega) + (1 - \sin^2 \theta \cos^2 \phi) S^{bb}(\mathbf{Q}, \omega) \\
& + (1 - \sin^2 \theta \sin^2 \phi) S^{cc}(\mathbf{Q}, \omega).
\end{aligned} \tag{1}$$

Here (θ, ϕ) are polar angles for wave vector transfer, \mathbf{Q} , ($\hat{\mathbf{Q}} \cdot \hat{\mathbf{a}} = \cos \theta$). In this experiment we report data for \mathbf{Q} in the $(hk0)$ and $(h0l)$ planes of the reciprocal lattice corresponding to $\phi = 0$ and $\phi = \pi/2$ respectively. Normalization of magnetic scattering intensities to the integrated intensity of acoustic phonons and assuming that $g=2$ allow us to report data in units of $1/\text{meV}$ defined such that $\int d^3\mathbf{Q} \int \hbar d\omega \sum_{\alpha} S^{\alpha\alpha}(\mathbf{Q}, \omega) / \int d^3\mathbf{Q} = S(S+1)$, where $S = 1$ is the spin quantum number for the Ni ions.

Our sample consists of two single crystals of Y_2BaNiO_5 with total mass 0.72g which were kept at $T=10\text{K}$ in a displac. The experiments were performed on the Pyrolytic Graphite (PG) based thermal neutron triple axis spectrometers BT2 and BT4 at NIST. We used the fixed final energy mode with $E_f=13.7\text{meV}$ and $E_f=14.7\text{meV}$ and a 2.5 cm thick PG filter before the analyzer. Apart from magnetic scattering, nuclear incoherent scattering and fast neutrons also contribute to the detector count rate. These background contributions varied from 2 to 4 counts per min. with Q and $\hbar\omega$ but, unlike the magnetic scattering, do not depend significantly on sample orientation ($\hat{\mathbf{Q}}$). Thus for each constant- \mathbf{Q} scan we subtracted the $\hat{\mathbf{Q}}$ -independent background determined from similar scans with the sample rotated sufficiently to eliminate magnetic scattering in the range of energies probed.

Fig. 1 shows two spectra for symmetry-related values of \mathbf{Q} corresponding to $\tilde{q} = \pi$. Magnetic neutron scattering at the magnetic zone center occurs only at finite $\hbar\omega$ which is evidence for the Haldane gap in this material. Both scans were performed for \mathbf{Q} in the $(hk0)$ zone ($\phi = 0$), but the angle, θ , between \mathbf{Q} and the chain axis is different for the two scans. The strongest peak in both scans is at $\hbar\omega \approx 9.8\text{meV}$. In Fig. 1 (a) where $\theta = 63^\circ$, a second peak appears at $\hbar\omega \approx 7.6\text{meV}$. The fact that this peak is not visible in Fig. 1 (b) where \mathbf{Q} is almost parallel to the chain axis ($\theta = 12^\circ$) proves that the 7.6meV mode is associated with magnetic fluctuations polarized along the chain axis (Eq. (1)). A previous neutron scattering experiment on a powder sample [19] showed an additional peak for $\hbar\omega = 16\text{meV}$.

Our data show that there is no peak in the magnetic scattering for $\hbar\omega = 16\text{meV}$ and $\tilde{q} = \pi$. The peak observed in the powder experiment could either be non-magnetic or could result from magnetic scattering at a different value of \mathbf{Q} .

The data in Fig. 1 also indicate that the two transverse modes are not degenerate. In Fig. 1(a) there is more intensity between 7.6 and 9.8meV than can be accounted for by two resolution limited modes. Moreover the peak in Fig. 1(b), which comes almost exclusively from transverse spin fluctuations, is much broader than our resolution. Additional evidence for the splitting of the transverse modes is provided by Fig. 2, where we compare higher resolution constant $\tilde{q} = \pi$ scans for $\phi = 0$ ((hk0) zone) and $\phi = \pi/2$ ((h0l) zone). According to Eq. (1) spin fluctuations perpendicular to the scattering plane always contribute to $I(\mathbf{Q}, \omega)$. Indeed, other things being equal, S^{cc} accounts for half of the spectral weight for any \mathbf{Q} in the (hk0) plane. A mixture of S^{aa} and S^{bb} accounts for the other half, implying that if \mathbf{Q} is neither along $\hat{\mathbf{a}}$ nor $\hat{\mathbf{b}}$, and if S^{aa} , S^{bb} and S^{cc} are peaked at resolvably different energies, S^{cc} will yield the most pronounced feature in $I(\mathbf{Q}, \omega)$. Similarly, S^{bb} will dominate $I(\mathbf{Q}, \omega)$ in the (h0l) plane. Clearly the strongest peak in $I(\mathbf{Q}, \omega)$ occurs at higher energy for (hk0) zone data than for (h0l) zone data. Inter-chain coupling cannot account for this energy shift since no corresponding shift is seen in the lowest energy longitudinal mode. Furthermore, the data labeled $\tilde{q}_b = 0$ and $\tilde{q}_c = 0$ in Fig. 2 were collected at equivalent values of \mathbf{Q} . We conclude that anisotropy transverse to the spin chain creates separate gaps at 8.8meV and 9.8meV for spin fluctuations along the \mathbf{b} and \mathbf{c} directions respectively.

Having determined the gap energies using constant- \mathbf{Q} scans, we performed constant- $\hbar\omega$ scans at higher energies to determine the velocity of spin excitations along the chain. The data are shown in Fig. 3. The peaks were fitted to gaussians whose positions are summarized in Fig. 4. From these data we estimate $v = \hbar\partial\omega(\tilde{q})/\partial\tilde{q} \approx 70(5)\text{meV}$ for $\tilde{q} \approx 1.1\pi$.

To extract accurate values of gaps and spin wave velocities and to determine whether the peaks are resolution limited, we compare the data to a model for the dynamic spin correlation function which is based on the ‘‘Single Mode Approximation’’ [26,27]

$$S^{\alpha\alpha}(\tilde{q}, \omega) = \frac{2}{3}(-\langle \mathcal{H} \rangle / L) \frac{1 - \cos \tilde{q}}{\hbar\omega_{\alpha}(\tilde{q})} \delta(\hbar\omega - \hbar\omega_{\alpha}(\tilde{q})). \quad (2)$$

For $\hbar\omega_{\alpha}(\tilde{q})$ we use the following form which was found to account for data in NENP [12] :

$$\hbar\omega_{\alpha}(\tilde{q}) = \sqrt{\Delta_{\alpha}^2 + v^2 \sin^2 \tilde{q} + A \cos^2 \frac{\tilde{q}}{2}}. \quad (3)$$

The solid lines in Figs. 1-3 are the result of a global fit of Eqs. (1-3) to all our data. The energies of the three gaps, the spin wave velocity, the ground state energy ($\langle \mathcal{H} \rangle / L$) and flat backgrounds for constant energy transfer scans were varied. Our data for $\tilde{q} \approx \pi$ is insensitive to the value of A so this parameter was fixed to 170meV². The value obtained by scaling A for NENP by the squared ratio of the mode averaged energy gap for the two materials. The reasonable overall agreement between the model (solid lines in Figs. 1-3) and data ($\chi^2 = 3.8$) indicates that the single mode approximation provides an acceptable description of dynamic spin correlations in Y₂BaNiO₅. The energies of the three modes obtained in this global fit are $\Delta_a = 7.7(1)$ meV, $\Delta_b = 8.8(1)$ meV and $\Delta_c = 9.8(1)$ meV. Note however that peaks in the data in general appear broader than predicted by the model (see eg Fig. 1(a) for $\hbar\omega \approx 8$ meV). This is surprising since experiments on other S=1 spin chains [12] and numerical simulation [6] indicate that the Haldane mode for $\tilde{q} \approx \pi$ and $k_B T \ll \Delta$ is long-lived. Likely causes for the broadened peaks are chain severing defects in our sample [16,20]. For an isolated chain with L Ni²⁺ spins, the energy of the lowest lying one-magnon state is approximately [7] $\Delta(L) = \sqrt{\Delta^2(\infty) + v^2 \sin^2(\pi(1 - 1/L))}$, where $\Delta(\infty)$ is the value of the gap for the infinite length chain. In a sample with a chain-severing defect concentration, c, there exists a Poisson distribution, $P(L) = Lc^2(1-c)^L$ of chains with different lengths, L, and hence a distribution of energy gaps. In addition there is quantization of \tilde{q} (in steps of $1/L$) for finite length chains. Given imperfect spectroscopic resolution, these effects broaden the peaks in $S(\tilde{q}, \omega)$. To determine their relevance to our experiment, we measured the magnetic susceptibility of a small fragment of our sample. Apart from the exponentially activated susceptibility associated with the Haldane gap, we found a Curie tail with a strength corresponding to $1.9 \pm 0.2\%$ spin-1/2 impurities per Ni²⁺ ion. Assuming that

a chain severing defect adds two spin-1/2 degrees of freedom [28–31], the concentration of such defects is $c = 1.0 \pm 0.1\%$. We then modeled $S(\tilde{q}, \omega)$ in a single finite-length spin chain by displacing the dispersion relation to the energy of the lowest lying one magnon mode, $\Delta(L)$, and convoluting with a gaussian in \tilde{q} with Full-Width at Half-Maximum (FWHM) $1/L$. To account for the random location of defects along the spin chains we summed dynamic correlation functions for the 10 most likely chain lengths weighted according to the Poisson distribution. Fitting to this model, which had no more adjustable parameters than the previous fit, yielded a significantly better fit to the data ($\chi^2 = 2.8$) as is apparent from the dashed lines in Figs. 1-3. Thus chain severing defects *could be* the reason for the broadening of peaks in constant- \tilde{q} scans observed in our sample [20]. The infinite chain length gap values derived from this fit were $\Delta_a = 7.5(1)\text{meV}$, $\Delta_b = 8.6(1)\text{meV}$ and $\Delta_c = 9.6(1)\text{meV}$. The average gap energy is $\bar{\Delta} = \frac{\Delta_a + \Delta_b + \Delta_c}{3} = 8.6(1)\text{meV}$.

We now discuss the implications of our experiment for the magnetic Hamiltonian of Y_2BaNiO_5 . The key result is the nearly isotropic nature of the Haldane gap in Y_2BaNiO_5 , which implies that to a very good approximation an appropriate starting point is that for an antiferromagnetic Heisenberg chain with exchange parameter $J \approx \bar{\Delta}/0.4105 = 21\text{meV}$ [7]. This value is about 20% lower than the value $|J| \approx 285\text{K} = 24.6\text{meV}$ deduced from susceptibility measurements [19]. The ratio of the gap to the spin wave velocity $\bar{\Delta}/v \approx 0.13$, which is close to the ratio of 0.16 in NENP [12]. Finally from the prefactor to the fit we obtain $\langle \mathcal{H}/LJ \rangle = -1.3 \pm 0.2$ which is close to the value -1.4015 ± 0.0005 [5] obtained from numerical calculations.

From our data, we can not distinguish between single-ion anisotropy and exchange anisotropy. If we assume, as is customary in the field, that exchange anisotropy can be neglected, the relevant anisotropy terms in the spin Hamiltonian are $DS_z^2 + E(S_x^2 - S_y^2)$ where x, y and z denote the b, c and a axis respectively. Numerical calculations [8] for the uniaxial $S=1$ chain ($E = 0$) show that $\Delta_{\perp} = \Delta_0 - 0.57D$ and $\Delta_{\parallel} = \Delta_0 + 1.41D$ where Δ_0 is the gap value in the absence of anisotropy. If we take Δ_{\perp} to be the average of the transverse mode energies in Y_2BaNiO_5 , we obtain $\Delta_0 \approx 8.6\text{meV}$ and $D \approx -0.81\text{meV}$ (easy-axis

anisotropy). For $D/J = 0.18$ the splitting of the transverse modes equals $4E$ [8]. Using this result to estimate a value for E in Y_2BaNiO_5 yields $E \approx 0.25\text{meV}$.

To determine the strength of interchain coupling along the b and c directions, we performed constant- $\tilde{q} = \pi$ scans varying the wave-vector components perpendicular to the chain. No dispersion is visible in our data (Fig. 2 and inset to Fig. 4) and this allows us to place an upper limit of 0.25 meV on any dispersion along these directions for $\tilde{q} = \pi$. An upper bound on the interchain couplings $J'_{b,c}$ is obtained using the classical spin-wave expression for the dispersion of the $\tilde{q} = \pi$ gap in a body-centered orthorhombic easy axis antiferromagnet [25]. We find $|J'_{b,c}| \leq \frac{(\Delta_0 + 0.25)^2 - (\Delta_0)^2}{2 \times 8 S^2 J} \approx 0.012\text{meV}$ so the ratio $|J'_{b,c}/J| \leq 5 \times 10^{-4}$. This is more than one order of magnitude smaller than the critical ratio $|J'/J| \approx 0.4/z'(\Delta_0/J)^2 \approx 1.3 \times 10^{-2}$ required to induce a magnetically ordered ground state [32,33]. Here $z' = 4$ is the chain coordination number corresponding to $J_{b,c}$. Note however that our data are insensitive to exchange coupling between the corner and body-centered Ni^{2+} ions because the effects of this frustrated interaction tend to cancel for $\tilde{q} \approx \pi$. Comparing different materials we have $D/J = -3.9 \times 10^{-2}$ and $|J'/J| < 5 \times 10^{-4}$ for Y_2BaNiO_5 whereas $D/J = -3.8 \times 10^{-3}$ and $|J'/J| = 2 \times 10^{-4}$ for CsNiCl_3 [9], $D/J = 0.18$ and $|J'/J| = 8 \times 10^{-4}$ for NENP [13], and $D/J = 5.8 \times 10^{-3}$ [34] and $|J'/J| \approx 10^{-5}$ for AgVP_2S_6 [14].

In summary, spin space anisotropy and interchain couplings are relatively weak perturbations in Y_2BaNiO_5 . They lead to splitting of the Haldane gap for $\tilde{q} = \pi$ into three modes at $\Delta_a = 7.5(1)\text{meV}$, $\Delta_b = 8.6(1)\text{meV}$ and $\Delta_c = 9.6(1)\text{meV}$ with less than 0.25meV dispersion for wave vector transfer perpendicular to the spin chains. The novel magnetic phenomena which occur in derivatives of this material thus take place in a system whose underlying Hamiltonian is that of a nearly perfect Heisenberg chain with antiferromagnetic interactions between neighboring $S=1$ ions.

JFD acknowledges the support of the Louisiana Board of Regents through the Louisiana Education Quality Support fund under contract number LEQSF(RF/1995-96)-RD-A-38. Work at JHU was supported by the NSF through DMR-9302065 and DMR-9453362.

REFERENCES

- [1] F. D. M. Haldane, Phys. Lett. **93A**, 464 (1983); Phys. Rev. Lett. **50**, 1153 (1983).
- [2] I. Affleck, *et al.*, Phys. Rev. Lett. **59**, 799 (1987).
- [3] D. P. Arovas, A. Auerbach, F. D. M. Haldane, Phys. Rev. Lett. **60**, 531 (1988).
- [4] M. den Nijs and K. Rommelse, Phys. Rev. **B40**, 4709 (1989).
- [5] M. P. Nightingale and H. Blöte, Phys. Rev. **B 33**, 659 (1986).
- [6] J. Deisz *et al.*, Phys. Rev. **B 42**, 4869 (1990). S. V. Meshkov, Phys. Rev. **B 48**, 6167 (1993).
- [7] S. R. White and D. A. Huse, Phys. Rev. **B 48**, 3844 (1993).
- [8] O. Golinelli, Th. Jolicoeur, and R. Lacaze, Phys. Rev. **B 45**, 9798 (1992); Phys. Rev. **B 50**, 3037 (1994).
- [9] R. M. Morra *et al.*, Phys. Rev. **B, 38**, 543 (1988)
- [10] W. J. L. Buyers *et al.*, Phys. Rev. Lett. **56**, 371 (1986).
- [11] J. P. Renard *et al.*, J. Appl. Phys. **63**, 3538 (1988).
- [12] S. Ma, *et al.*, Phys. Rev. Lett. **69**, 3571 (1992).
- [13] L. P. Regnault *et al.*, Phys. Rev. **B, 50**, 9174 (1994)
- [14] H. Mutka *et al.*, Phys. Rev. **B39**, 4820 (1989).
- [15] St. Schiffler and Müller-Buschbaum, Z. Anorg. Allg. Chem. **532** 10 (1986).
- [16] J. F. DiTusa *et al.*, Phys. Rev. Lett., **73**, 1857 (1994)
- [17] K. Kojima *et al.*, Phys. Rev. Lett. **74**, 3471 (1995).
- [18] A. Zheludev *et al.*, unpublished (1996).

- [19] J. Darriet and L. P. Regnault, *Solid State Comm.* **86**, 409 (1993).
- [20] J. F. DiTusa *et al.*, *Physica B* **194-196**, 181-182 (1994).
- [21] T. Yokoo *et al.*, *J. Phys. Soc. Jap.* **64**, 3651 (1996).
- [22] We recently received a preprint from T. Sakaguchi *et al.* which arrives at conclusions similar to ours.
- [23] E. Garcia-Matres *et al.*, *J. Solid State Chem.*, **103**, 322 (1993); D. J. Buttrey *et al.*, *J. Solid State Chem.*, **88**, 291 (1990).
- [24] N. D. Chesser and J. D. Axe, *Acta Crystallogr. Sect.A* **29**, 160 (1973).
- [25] S. W. Lovesey, *Theory of Neutron Scattering from Condensed Matter*, Clarendon Press, Oxford (1984).
- [26] R. P. Feynmann, *Statistical Mechanics*, Chap. 11, Benjamin, Reading, Mass., (1972).
- [27] S. M. Girvin, A. H. MacDonald, P. M. Platzman, *J. Magn. Magn. Mater.* vol.**54-57**, pt.3, 1428 (1985)
- [28] T. Kennedy, *J. Phys. Condens. Matter* **2**, 5737 (1990).
- [29] A. P. Ramirez *et al.*, *Phys. Rev. Lett.*, **72**, 3108 (1994).
- [30] S. H. Glarum *et al.*, *Phys. Rev. Lett.* **67**, 1614 (1991).
- [31] P. P. Mitra *et al.*, *Phys. Rev. B*, **45**, 5299 (1994).
- [32] T. Sakai and M. Takahashi, *Phys. Rev. B* **42**, 1090 (1990); *ibid* **42**, 4537 (1990).
- [33] Y. A. Kosevich and A. V. Chubukov, *Sov. Phys. JETP* **64**, 654 (1986).
- [34] M. Takigawa *et al.*, *Phys. Rev. Lett.* **76**, 2173 (1996); *Phys. Rev. B***52**, R13087 (1995).

FIGURES

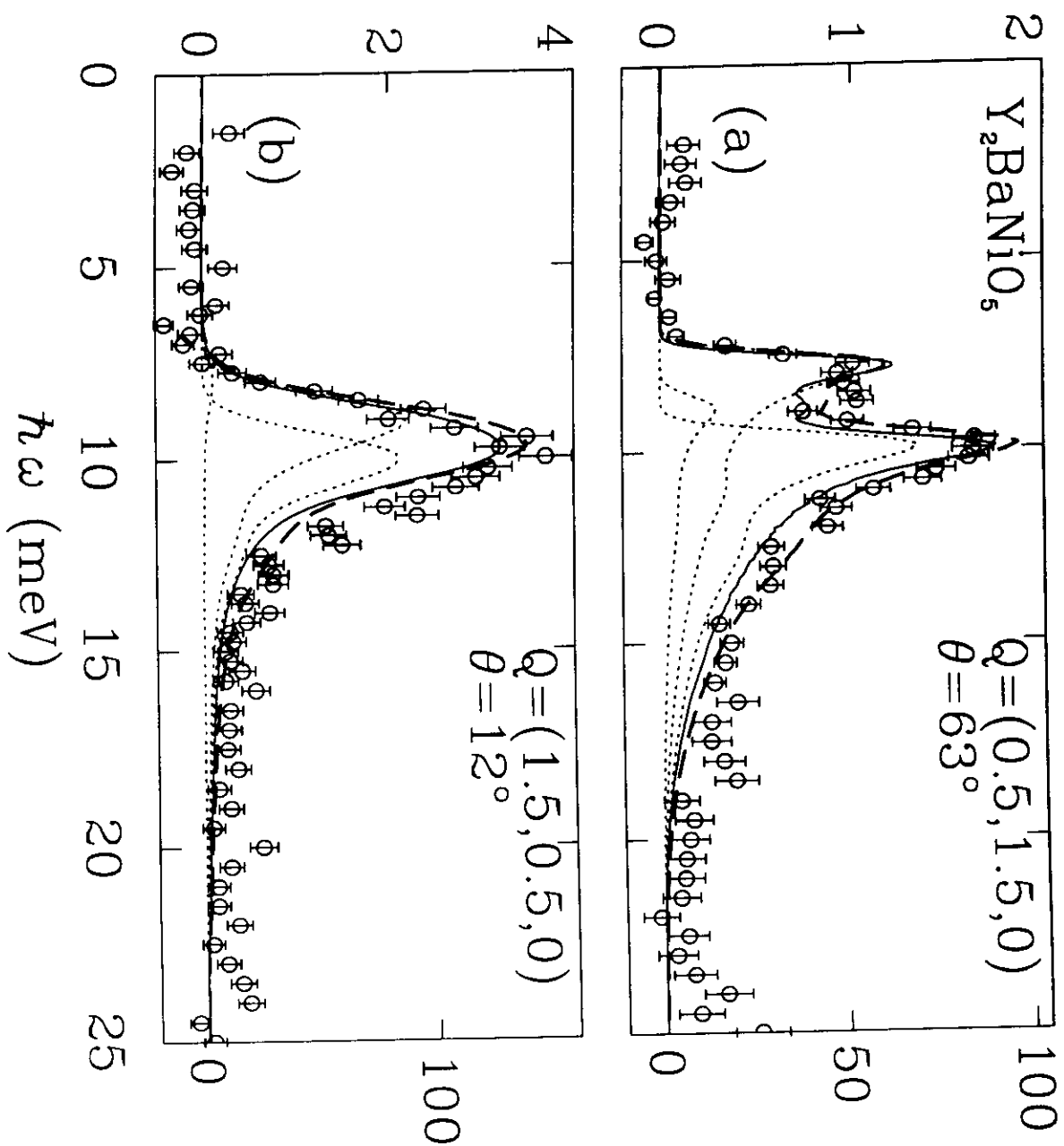
FIG. 1. Background subtracted constant- \mathbf{Q} scans. Collimations were $40^\circ\text{-}40^\circ\text{-}40^\circ\text{-}80^\circ$ and $E_f=14.7\text{meV}$ on BT4. At $\hbar\omega = 10\text{meV}$, the FWHM energy resolution is $\Delta E = 1.6\text{meV}$ while the wave-vector resolutions along the chain are $\Delta\tilde{q}/\pi = 0.110$ and 0.048 for frames (a) and (b) respectively. Solid lines are from the global fit. Dashed lines include the effects of a chain severing defect density of 1%. Dotted lines show contributions from each mode of polarization.

FIG. 2. Background subtracted constant- \mathbf{Q} scans in the $(hk0)$ (top frame), and $(h0l)$ (bottom frame) zones where $\phi = 0$ and $\pi/2$ respectively (see Eq. (1)). Wave vector transfer from top to bottom was $(0.5,2,0)$, $(0.5,1.5,0)$, $(0.5,0,2)$ and $(0.5,0,2.5)$. Collimations were $20^\circ\text{-}20^\circ\text{-}40^\circ\text{-}100^\circ$, and $E_f=13.7\text{meV}$ on BT2. At $\hbar\omega = 10\text{meV}$, the energy resolution was 1.07meV (FWHM) and the wave vector resolutions along the chain are $\Delta\tilde{q}/\pi = 0.08, 0.104, 0.060,$ and 0.040 , respectively (from top to bottom). Solid and dashed lines are described in the caption to Fig. 1.

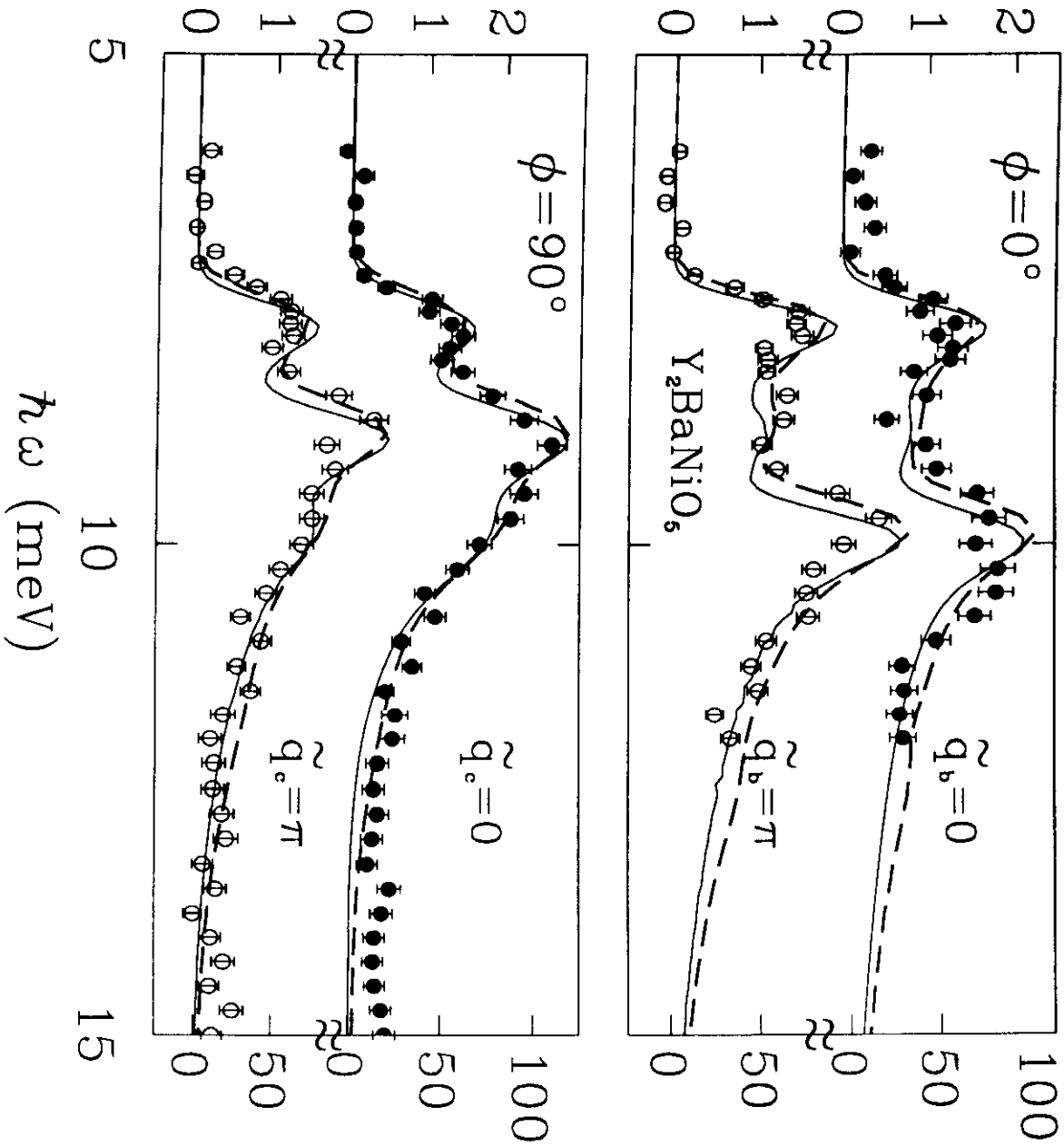
FIG. 3. Constant energy transfer scans with collimations $60^\circ\text{-}20^\circ\text{-}40^\circ\text{-}100^\circ$, $60^\circ\text{-}20^\circ\text{-}40^\circ\text{-}100^\circ$, $40^\circ\text{-}40^\circ\text{-}40^\circ\text{-}80^\circ$ and $20^\circ\text{-}20^\circ\text{-}40^\circ\text{-}100^\circ$; fixed final energies E_f of $13.7, 13.7, 14.7$ and 13.7meV ; energy resolutions (ΔE) of $2.75, 2.31, 2.10$ and 1.04meV ; and wave vector resolutions ($\Delta\tilde{q}/\pi$) along the chain of $0.04, 0.04, 0.04$ and 0.034 , respectively (from top to bottom). Solid and dashed lines are described in the caption to Fig. 1.

FIG. 4. Dispersion relation for magnetic excitations in Y_2BaNiO_5 . The lines are our best estimate of the dispersion relation for infinite length spin chains obtained from a global fit to all data taking into account resolution effects and 1% chain severing defects in our sample. The points for $\tilde{q} = \pi$ were obtained through fits of the same model to single constant \tilde{q} scans. The points at higher energies were obtained by gaussian fits to the data in Fig 3. The inset shows the dependence of the $\tilde{q} = \pi$ energy gaps on wave vector transfer $\tilde{q}_{\perp b} = 2\pi k$ (open symbols) and $\tilde{q}_{\perp c} = 2\pi l$ (filled symbols).

$I(\tilde{q}, \omega)$ (1/meV)



$I(\tilde{q}, \omega)$ (1/meV)



Δ Intensity (Counts pr 15min)

